

NONHOLONOMIC, BOUNDED CURVATURE PATH PLANNING IN CLUTTERED ENVIRONMENTS

Corrado Santilli, Antonio Bicchi, Giuseppe Casalino, and Aldo Balestrino

*DSEA - Dipartimento di Sistemi Elettrici ed Automazione &
Centro "E. Piaggio"
via Diotisalvi, 2. 56100 Pisa, Italia
Tel.:(39)50-565328; Fax:(39)50-565333; Email: bicchi@dsea.unipi.it
Università di Pisa*

Abstract

The problem of planning a path for a robot vehicle amidst obstacles is considered. The kinematics of the vehicle being considered are of the unicycle or car-like type, i.e. are subject to nonholonomic constraints. Moreover, the trajectories of the robot are supposed not to exceed a given bound on curvature, that incorporates physical limitations of the allowable minimum turning radius for the vehicle. The presented method attempts at extending Reeds and Shepp's results on shortest paths of bounded curvature in absence of obstacles, to the case where obstacles are present in the workspace. The method does not require explicit construction of the configuration space, nor employs a preliminary phase of holonomic trajectory planning. Successful outcomes of the proposed technique are paths consisting of a simple composition of Reeds/Shepp paths that solves the problem. For a particular vehicle shape, the path provided by the method, if regular, is also the shortest feasible path. In its original version, however, the method may fail to find a path, even though one may exist (path-completeness not guaranteed). Most such empasses can be overcome by use of a few simple heuristics suggested in the text. Applications to both unicycle and car-like (bicycle) mobile robots of general shape are described and their performance and practicality discussed.

1 Introduction

Motion planning for nonholonomic vehicles is attracting a wide interest in Robotics because of both its application potentials (automated factories and highways, assisted parking maneuvering, etc.) and its theoretical challenges. One of the interesting features of this field is that its background is composed of work done in holonomic motion planning (a predominantly A.I. area) and in nonlinear systems theory.

A nonholonomic constraint is a non integrable equation involving the configuration parameters and their derivatives (velocity parameters). Such constraints do not reduce the dimension of the robot configuration space (like holonomic constraints do), but reduce the dimension of the velocity space at any given configuration. Thus, a kinematic model of a car-like vehicle can be parked everywhere in a free three-dimensional workspace, although it only possesses two control inputs. This comes at the price of more complex planning for maneuvers such as parallel parking. In the case that obstacles are present, it has been shown by Barraquand and Latombe [1990] the non-trivial fact that a car with curvature limitations moving amidst obstacles remains fully controllable, that is, whenever a free (holonomic) trajectory exists, the existence of a feasible path is also guaranteed.

The presence of lower bounds on the minimum turning radius involves curvature constraints on feasible trajectories that deeply affect the geometry of the problem. The problem of finding the shortest path between two configurations in the plane with curvature limitations is an interesting geometric problem *per se*, that was solved first by Dubins [1957] for smooth trajectories. Only recently, Reeds and Shepp [1990] solved the geodesic problem when reversals are allowed. They have shown that a path with shortest length can always be built by concatenating at most five linear or circular segments, including at most two cusps. The radius of circular segments is the minimum allowed turning radius, and cusps correspond to reversals. The same result has recently been derived again by Sussmann and Tang [1991] and Boissonnat, Cerezo, and Leblond [1992], using Pontryagin's maximum principle. These theoretical results ignited a new series of methods tending to find shortest nonholonomic paths with bounded curvature amidst obstacles, among which [Jacobs and Canny, 1989], [Jacobs, Laumond, Taix and Murray, 1991], [Mirtich and Canny [1992].

The method presented in this paper is also inspired by Reeds and Shepp's work. The path resulting is a simple concatenation of linear and circular segments, the latter having minimum turning radii. The principal worth of the method is in its simplicity and in the regularity of the resulting paths. Although the method is reminiscent of several others proposed in literature, it does not seem to have been discussed in this form for nonholonomic vehicles. In particular, the method can be regarded as a generalization of visibility graph methods, to which it reduces as bounds on path curvature are lifted.

This paper reports on preliminary results in the implementation of the method, and leaves some important questions open. The method is not path-complete, although simple heuristics can help in solving most of the typical deadlocks encountered. Nevertheless, the optimality of visibility graph solutions is partially inherited by the proposed method when applied to the particular case of a circular robot. Taking this as a hint, the algorithm can be applied to more general types of mobile robots. Simulation results are reported in this paper, that support such an extension as one providing very reasonable paths.

2 The proposed planner

Fig.1-a shows a mobile robot, modelled as a two dimensional object \mathcal{A} moving in a 2-dimensional workspace. The configuration space of the robot is $\mathbf{R}^2 \times \mathbf{S}^1$, and can be parameterized by the coordinates x and y of the robot reference point P , and by the angle

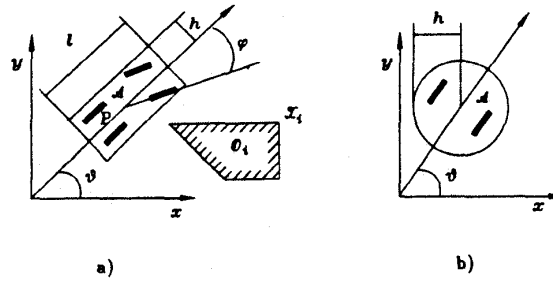


Figure 1: A generic car-like robot (a) and a particular unicycle vehicle (b).

θ (representing the robot orientation) between the x -axis of the base frame \mathcal{F}_S and the main axis of the robot. The robot shape is assumed symmetric with respect to its main axis, and its half-width is denoted by h . We restrict ourselves to consider only polygonal obstacles in the workspace, that we indicate with \mathcal{O}_i , $i = 1, \dots, l$, while their n vertices are listed in \mathcal{X}_j , for $j = 0$ to n . A nonholonomic constraint arises because the wheels can roll and spin but not slip, hence the robot cannot move sidewise. For a unicycle vehicle such as that shown in fig.1-b, the nonholonomic constraint is written as

$$S(\mathbf{q})\dot{\mathbf{q}} = \begin{bmatrix} -\sin(\theta) & \cos(\theta) & 0 \end{bmatrix} \begin{bmatrix} \dot{x} \\ \dot{y} \\ \dot{\theta} \end{bmatrix} = 0$$

The motion planning problem can be stated as follows:

Problem 1 Let $\mathbf{q}_s = (x_s, y_s, \theta_s)$ and $\mathbf{q}_g = (x_g, y_g, \theta_g)$ be respectively the initial and final configuration of a robot \mathcal{A} with minimum turning radius ρ_{min} and half-width h . Determine a path $\bar{\mathbf{q}}(\tau)$ that minimizes the cost functional

$$L(\bar{\mathbf{q}}(\cdot)) \stackrel{def}{=} \int_0^T \sqrt{x'^2(\tau) + y'^2(\tau)} d\tau, \quad (1)$$

subject to

$$\bar{\mathbf{q}}(0) = \mathbf{q}_s; \quad (2)$$

$$\bar{\mathbf{q}}(1) = \mathbf{q}_g; \quad (3)$$

$$\mathcal{A}(\bar{\mathbf{q}}(\tau)) \cap \mathcal{O}_i = \emptyset \quad i = 1, \dots, l, \quad \forall \tau \in [0, 1]; \quad (4)$$

$$S(\bar{\mathbf{q}})\bar{\mathbf{q}}'(\tau) = 0, \quad \forall \tau \in [0, 1]; \quad (5)$$

$$\bar{\mathbf{q}}(\tau) \in C^1, \text{ and } \frac{x'y'' - x''y'}{(x'^2 + y'^2)^{3/2}} \leq \frac{1}{\rho_{min}}, \quad (6)$$

where $\bar{\mathbf{q}}' = \frac{d\bar{\mathbf{q}}(\tau)}{d\tau}$, $x' = \frac{dx(\tau)}{d\tau}$, $y' = \frac{dy(\tau)}{d\tau}$, $x'' = \frac{d^2x(\tau)}{d\tau^2}$, $y'' = \frac{d^2y(\tau)}{d\tau^2}$.

Finding a solution for this problem is in general quite difficult. In this paper we introduce an algorithm that exhibits some interesting properties when considering the particular type of mobile robot shown in fig.1-b, and that can be extended to more general cases.

Algorithm 1 a) Draw n circles with radius $\rho = \max\{\rho_{min}, h\}$ centered in the vertices of the obstacles. Also draw two circles with radius ρ_{min} passing through $[x_s, y_s]$ and tangent to the line through $[x_s, y_s]$ with angle θ_s , and an analogous pair of circles for the final configuration \mathbf{q}_g .

- b) Consider the $n+4$ circles two at a time, and draw the four linear segments belonging to the common tangent lines and comprised between the tangency points. Also consider all arcs on circles that join any two tangency points. Let a basic path diagram (BPD) be composed of two directed segments for each of these linear and circular segments.
- c) The basic path diagram may contain non-free paths, that is, paths that cannot be followed by the robot without colliding with obstacles. Directed segments are then tested singularly and those causing collisions are eliminated from the diagram. In general, a segment may be free if followed in one sense, but not otherwise. For robots that are symmetric with respect to a line through the reference point and normal to the main axis of the robot, the direction of motion along a path is not relevant, and a simpler basic path diagram can be considered.
- d) A directed graph G is built from the thus emended path diagram (EPD) as follows:
- the start and goal configurations are nodes of G ;
 - for all points of tangency between a linear and a circular segment, two configurations (corresponding to the possible orientations aligned with the common tangent direction) are nodes of G ;
 - two nodes i and j of G are connected with an oriented link from i to j if the corresponding directed segment on the emended path diagram exists;
 - a cost equal to the length of the corresponding segment is associated to each link.
- e) The directed graph G is searched for a path from the start to the goal configuration using the length of the overall path as the cost function.

The above mentioned property of this algorithm is formalized in the following

Theorem 1 For a circular mobile robot A with radius h equal to the minimum turning radius ρ_{min} moving in a bidimensional polygonal workspace S , a sufficient condition for a path to be the solution of problem 1 is that it is a regular output of algorithm 1.

The proof is based on the application of techniques of optimal control in bounded phase spaces, that show that optimal trajectories (if any exists) are compositions of segments of lines and of circles of minimal radius, along with pieces of the boundary of obstacles in configuration space. In the specific case of the circular robot under consideration, also obstacle boundaries are built of such segments. Finally, generalized visibility graph arguments are used to obtain the thesis. A detailed proof is reported in [Bicchi, Santilli, and Casalino, 1995]. The geometric reasoning behind the second part of the proof is reported below.

The configuration space \mathcal{V} associated with a circular robot contains C-obstacles that are generalized straight cylinders. In this case, the orientation parameter θ does not play a role in verifying holonomic constraints (4), nor does it influence the cost functional (1). Consider a two-dimensional configuration space \mathcal{V}' where C-obstacles are built simply by isotropically growing the obstacles in S by ρ . Fig.2 shows the workspace S (a) and the corresponding 2D configuration space \mathcal{V}' (b) in a simple example. Let P denote the set of free paths (i.e., triples $(x(\cdot), y(\cdot), \theta(\cdot))$ satisfying (4)) in \mathcal{V} , and P' be the corresponding set of $(x(\cdot), y(\cdot))$ pairs. Consider the visibility diagram V_d associated with \mathcal{V}' (fig.3-a), and the modified diagram W_d (fig.3-b). The latter differs from V_d because two "phantom" circular obstacles of radius ρ and tangent to the initial direction at q_s , and two analogous obstacles at q_g , are considered (see fig.3-b). Start and goal phantom obstacles influence

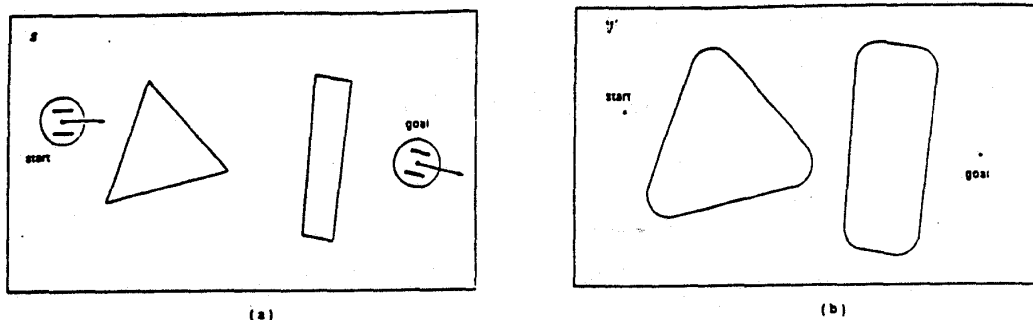


Figure 2: Workspace (a) and corresponding 2D configuration space (b) illustrating Theorem 1.

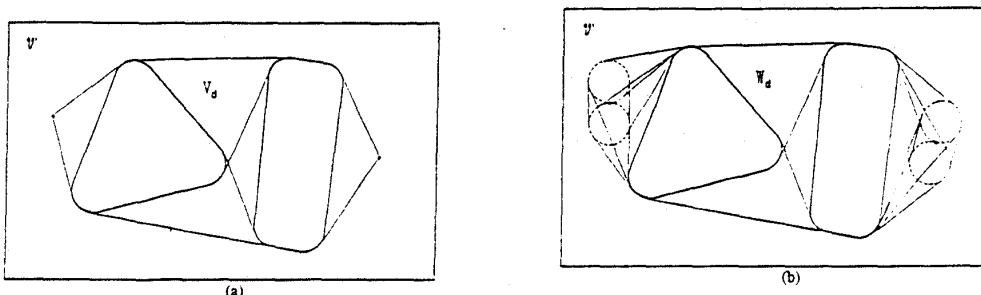


Figure 3: Extended visibility diagram without (a) and with "phantom" obstacles (b) for the example of fig. 2.

the visibility between two points only if either point is q_s , respectively q_g . Note that paths in V_d but not in W_d do not satisfy the constraint on curvature (6).

The BPD (and hence the EPD) built by algorithm 1 for the circular robot in S coincides with the modified visibility diagram W_d by construction. Therefore, if the path obtained by algorithm 1 on the EPD is regular (i.e., it contains no cusps), this is also the shortest path on W_d , and hence the shortest path in V_d subject to (6). From the properties of generalized visibility diagrams, the optimality of this path in P' subject to (6) follows. On the other hand, for every path in P' a corresponding path in P with $\theta(\tau) = \arctan \left[\frac{dy(\tau)}{dx(\tau)} \right]^{-1}$ (where the indeterminacy of the $\arctan(\cdot)$ function is solved by continuity) exists that satisfy the nonholonomic constraint (5). Such path is the optimal solution to Problem 1, and corresponds to the path obtained by Algorithm 1.

3 Discussion

Theorem 1 is probably one of the first attempts in literature at solving the optimal path planning problem 1. However, it only provides sufficient results in a very particular case. In this section we list some of the pitfalls of the proposed method along with simple heuristics that may help in applying the algorithm to more realistic robots.

Remark 1. Note that only sufficiency results have been established because of two facts:

- If algorithm 1 results in a path that contains reversals, visibility graph arguments can not be applied in the proof. Piecewise optimality of paths between reversals

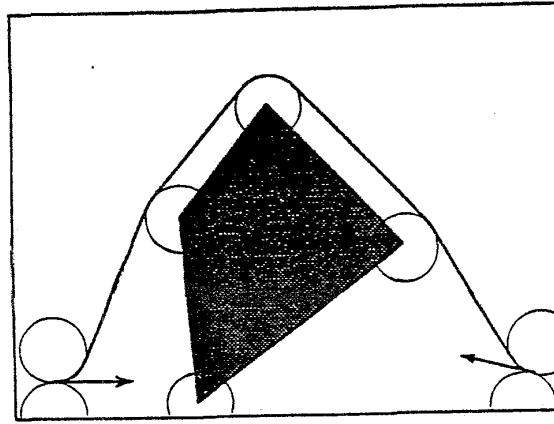


Figure 4: Impossibility to maneuver with too few obstacles.

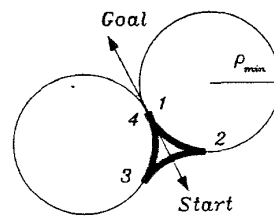


Figure 5: A Reeds/Shepp inversion pattern (a) can be introduced to solve the deadlock of fig 4 (b).

can still be argued, but Reeds/Shepp techniques are probably necessary to discuss global optimality.

- The method is not path-complete. For the circular robot of concern in theorem 1, incompleteness may be caused by the impossibility to maneuver without the support of an obstacle vertex. Consider for instance the case depicted in fig. 4, where the robot can use neither any of the obstacle circles to make the necessary reversal, nor the start and goal pairs of circles because of space limitations. A simple heuristic solution to this problem is to find a cell in free space where a Reeds/Shepp inversion pattern (see fig. 5-a) can be accommodated for, and to consider the corresponding additional pair of circles in the algorithm. In building the Reeds/Shepp inversion pattern, existing circles are considered first, as this usually requires less clearance. In fig. 5-b, the problem in fig. 4 is solved. Notice that introduction of auxiliary circles produces a graph G' that includes the original graph G , hence the search on G' provides a path whose length is at least equal to the shortest path on G .

In fact, a characteristic of the proposed algorithm is its suitability to highly cluttered environments, where it accomplishes its best performance. The method's weaknesses are more evident when the scarceness of obstacles does not offer support to enough circles and, therefore, maneuver possibilities. An instance of such a problem is put into evidence by the parallel parking problem. In fact, the proposed algorithm can park a circular robot of radius R if the clearance is larger than three times R , while from the above mentioned controllability results we know that parking is theoretically possible in slots just larger than $2R$. There is probably no easy fix to this problem,

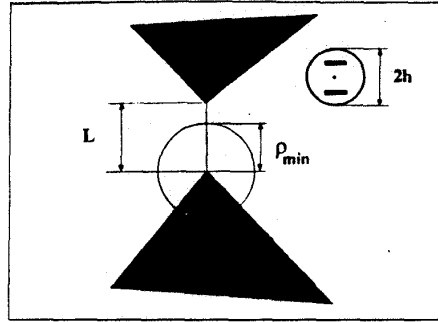


Figure 6: A possible deadlock for the algorithm

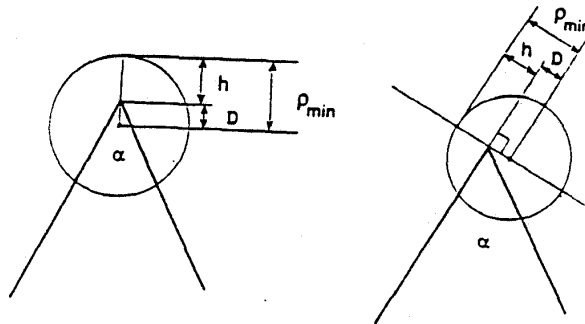


Figure 7: Modifications to the method to fix the deadlock in fig. 6

as its solution is only possible by approximating a non-feasible trajectory with a very high number of nonholonomic maneuvers (this is actually what the method of Jacobs *et al.* [1991] does in this case).

Remark 2.

If $\rho_{min} \neq h$, the circular segments of BPD are drawn with radius $\rho = \max \rho_{min}, h$. If $\rho_{min} < h$, the algorithm is applied similarly, except for circles at the start and goal, that are drawn with radius ρ_{min} . The optimality properties of algorithm 1 are still retained in this case. Also Reeds/Shepp inversion patterns can be introduced, if necessary, using circles of radius ρ_{min} .

If $\rho_{min} > h$, path-completeness of the method is further reduced in cases such as that depicted in fig. 6, where the vertex-to-vertex distance L is such that $2 * h < L < h + \rho_{min}$. An heuristic fix to this problem consists in replacing the circle drawn at each vertex with three circles of the same radius ρ_{min} . The center of the first circle lies on the bisector of the angle between the edges concurring in \mathcal{X}_i , at a distance $D = \rho_{min} - h$ from the vertex (see fig. 7-a). The centers of the second and third circles lie on the lines normal in \mathcal{X}_i to the obstacle edges, at a distance $D = \rho_{min} - h$ (fig. 7-b). The rationale behind this heuristic is that the three circles approximate the envelope to the family of paths that “graze” the obstacle vertex. In fact, such envelope provides the shortest path on the extended visibility diagram (not necessarily the shortest bounded curvature path).

Remark 3. For a polygonal vehicle, the proposed algorithm and heuristics can be applied

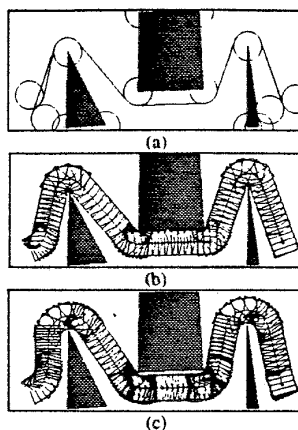


Figure 8: Planning the path of a Labmate with different turning radii. a) EPD for $\rho_{min} = h$; b) corresponding path; c) path corresponding to $\rho_{min} = 1.5h$.

without major modifications obtaining qualitatively good results, as it has been verified in a number of simulations and experiments. The latter were made using a LABMATE robot of Transition Research, Inc. (note that the LABMATE does not actually have lower bounds on the turning radius, that however have been simulated imposing software constraints). Consider for instance the simple planning problem for a Labmate in the environment depicted in fig. 8. The EPD obtained assuming $\rho_{min} = h$ is reported in fig. 8-a. Note that, due to the axial symmetry of the Labmate, all segments in EPD can be followed either way. In fig. 8-b the corresponding shortest path on the EPD is shown. Finally, fig. 8-c shows the path resulting from application of the heuristic discussed in remark 2 in the case that $\rho_{min} = 1.5h$. Note that, in spite of the considerable increase of the minimum turning radius, the path is still very close to the intuitive optimum. The described path planner can also provide a solution for car-like robots, i.e. vehicles whose nonholonomic constraint equation involves the steering angle ϕ and is of the form

$$S(\mathbf{q})\dot{\mathbf{q}} = \begin{bmatrix} -\sin(\theta) & \cos(\theta) & 0 & 0 \\ -\sin(\theta + \phi) & \cos(\theta + \phi) & w \cos(\phi) & 0 \end{bmatrix} \begin{bmatrix} \dot{x} \\ \dot{y} \\ \dot{\theta} \\ \dot{\phi} \end{bmatrix} = 0$$

The EPD of a parallel parking maneuver is reported in fig. 9-a (orientation of segments is not shown). The parking maneuver provided seems very natural, as shown in fig. 9-b. More complex planning problems for a car-like vehicle are shown in fig. 10. Note that, as compared to most current path planners, the proposed method behaves particularly well in much cluttered environments.

4 Conclusions

In this paper we have discussed a planning algorithm for nonholonomic, bounded curvature path planning among obstacles whose output is the shortest feasible regular path for a particular vehicle. Although the proposed method is not complete, nor its optimality properties are trivially carried over to more general vehicles, very reasonable paths are generated by using only a few additional simple heuristics.

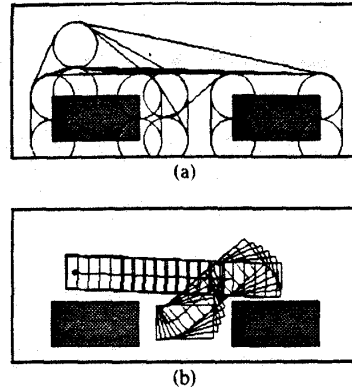


Figure 9: EPD (a) and final path (b) for the parallel-parking maneuver of a car-like vehicle.

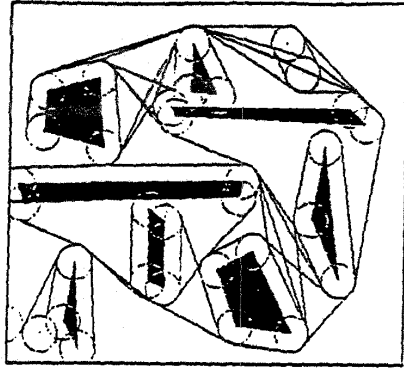
As compared with other methods known in the literature, the proposed planner does not need to build a supporting free path by means of configuration space methods nor does it require discretization of the configuration space. Paths generated by our method are typically very simple concatenations of Reeds/Shepp paths. An important quality of the proposed method is that it can be easily implemented even in cluttered workspaces, where the method actually performs comparatively best.

Acknowledgement

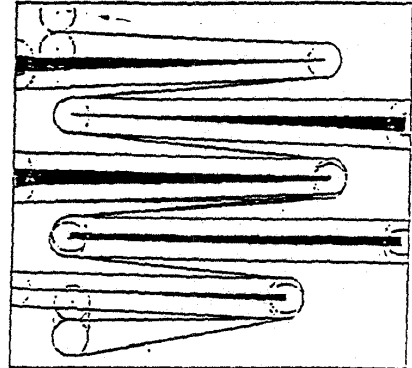
The research reported in this paper has been partially supported by the C.N.R. - Progetto Finalizzato Robotica under contract 93.01079.PF67.

References

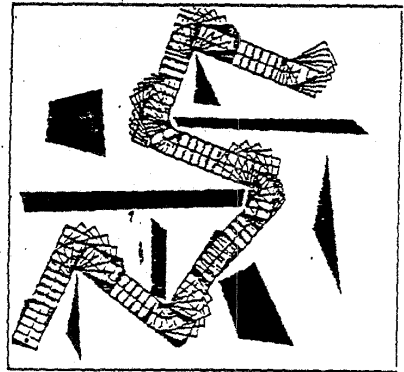
- J. Barraquand, J.C. Latombe: "Controllability of Mobile Robots with Kinematic Constraints", Technical Report No. STAN-CS-90-1317, Dept. of Computer Science, Stanford University, 1990.
- J.D. Boissonnat, A. Cerezo, and J. Leblond: "Shortest Paths of Bounded Curvature in the Plane", Proc. IEEE Int. Conf. on Robotics and Automation, pp.2315-2320, 1992.
- L. E. Dubins: "On curves of minimal length with a constraint on average curvature and with prescribed initial and terminal positions and tangents", *American Journal of Mathematics*, 79:497-516, 1957.
- P. Jacobs, J. Canny: "Planning Smooth Paths for Mobile Robots", *IEEE International Conference on Robotics and Automation*, AZ, 2-7, 1989.
- P. Jacobs, J. P. Laumond, M. Taix and R. Murray: "Fast and Exact Trajectory Planning for Mobile Robots and Other Systems with Nonholonomic Constraints", Technical Report 90318, LAAS/CNRS, Toulouse, France, September 1990.
- B. Mirtich, J. Canny: "Using Skeletons for Nonholonomic Path Planning among Obstacles", *IEEE International Conference on Robotics and Automation*, pp. 2533-2540, May 1990.
- J. A. Reeds, R. A. Shepp: "Optimal Paths for a Car that Goes both Forward and Backward", 145(2), 1990.
- H. J. Sussmann and G. Tang: "Shortest Paths for the Reeds-Shepp Car: a Worked Out Example of the Use of Geometric Techniques in Nonlinear Optimal Control", SYCON report 91-10, 1991.



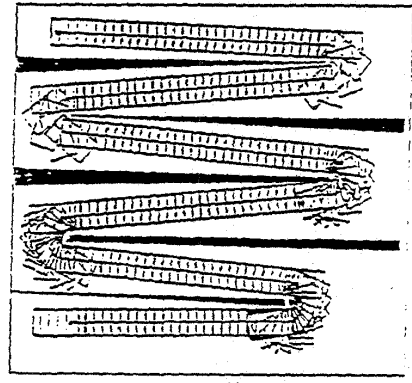
(a)



(a)



(b)



(b)

Figure 10: EPD's (a,c) and resulting paths (b,d) for a car-like vehicle in cluttered environments.